Preclinical evidence that 3'-Deoxy-3'-[^{18}F]Fluorothymidine PET can visualize recovery of hematopoesis after gemcitabine chemotherapy

[1] Sonja Schelhaas, [1,*] Annelena Held, [2] Nicole Bäumer, [1,**] Thomas Viel, [1] Sven Hermann, [2,3] Carsten Müller-Tidow, and [1,4] Andreas H. Jacobs

[1] European Institute for Molecular Imaging (EIMI), Westfälische Wilhelms-Universität (WWU) Münster, Münster, Germany

[2] Department of Medicine A, Molecular Hematology and Oncology, University Hospital of Münster, Münster, Germany

[3] Department of Internal Medicine, Hematology and Oncology, University of Hospital Halle, Germany

[4] Department of Geriatric Medicine, Johanniter Hospital, Bonn, Germany

* present address: Department of Orthopedic Surgery, Otto-von-Guericke University, Magdeburg, Germany

** present address: PARCC INSERM-U970, Université Paris Descartes, Paris, France

running title: [^{18}F]FLT PET imaging of hematopoiesis

key words: [^{18}F]FLT PET, hematopoiesis, myelosuppression

financial support: The research leading to these results has received support from the Innovative Medicines Initiative Joint Undertaking (www.imi.europa.eu) under grant agreement number 115151, resources of which are composed of financial contribution from the European Union's Seventh Framework Programme (FP7/2007-2013) and EFPIA companies' in kind contribution. This work was also supported by

the Deutsche Forschungsgemeinschaft (DFG), Cells-in-Motion Cluster of Excellence (EXC1003 – CiM), University of Münster.

Corresponding author:

Prof. Dr. med. Andreas H. Jacobs

European Institute for Molecular Imaging (EIMI)

Waldeyerstr. 15

48149 Münster

Germany

Phone: +492518349300

Fax: +492518349313

Email: ahjacobs@uni-muenster.de

conflict of interest: The authors disclose no potential conflicts of interest.

word count: 3565

number of figures: 5

number of tables: 0

number of supplementary figures: 4

number of supplementary tables: 3

ABSTRACT

Molecular imaging with the positron emission tomography (PET) tracer 3'-deoxy-3'-[^{18}F]fluorothymidine ([^{18}F]FLT) allows assessment of the proliferative state of organs *in vivo*. While used primarily in the oncology clinic, it can also shed light on the proliferation of other tissues, as demonstrated here for monitoring hematopoietic organs that recover after myelosuppressive chemotherapy. In the NMRI nude mouse model, we observed up to a 4.5-fold increase in [^{18}F]FLT uptake in bone marrow and spleen on d2, d3 and d5 after treatment with gemcitabine, a chemotherapeutic agent that is powerfully myelosuppressive in the model. Specifically, we observed (i) a reduced spleen weight; (ii) reduced bone marrow cell counts and proliferation (BrdU flow cytometry, spleen immunohistochemistry; 6 h / d1); and (iii) reduced leukocytes in peripheral blood (d5). In conclusion, our results show how [^{18}F]FLT PET can provide a powerful tool to non-invasively visualize the proliferative status of hematopoietic organs after myelosuppressive therapy.

INTRODUCTION

Chemotherapy of malignant cancers is frequently accompanied by several side effects. One of the most common adverse effects is the impact of the chemotherapeutic agent on bone marrow cells subsequently affecting the numbers of white blood cells (leukopenia or neutropenia (1)), platelets (thrombocytopenia (2)) and red blood cells (anemia (3)). For instance, neutropenia may result in secondary infections, ultimately leading to the death of the patient. It is well recognized that the hematopoietic organs are able to regenerate after insult due to the presence of hematopoietic stem cells. Therefore, it is of importance, not to employ a chemo- or radiotherapy in the phase of recovery of the hematopoietic organs, since this might result in destruction of hematopoietic stem cells with permanent impact on the blood composition. A range of models exist that describe the relation of the application of a chemotherapeutic agent and the impact on bone marrow and other tissues (4). To know this relation is of crucial importance for dosing and timing of a chemotherapeutic drug. Unfortunately, changes in the blood cellular components, which are easily measurable in clinical routine, are not directly timely linked to changes in the proliferation of hematopoietic stem cells.

Positron emission tomography (PET) is an attractive tool to non-invasively and longitudinally visualize molecular changes within a living organism. It is widely used in the fields of oncology, cardiology, and neuroscience. Depending on the radiotracer used it can monitor specific molecular events. 3'-deoxy-3'-[^{18}F]fluorothymidine ([^{18}F]FLT) is a thymidine analog that is transported into cells primarily via the human equilibrative nucleoside transporter 1 (hENT1, (5)). Within a cell, it is phosphorylated by thymidine kinase 1 (TK1) which results in trapping of the tracer. Hence, accumulation of [^{18}F]FLT resembles the thymidine salvage pathway and therefore proliferation. An alternative thymidine-to-DNA pathway is the *de novo* synthesis

pathway, with the key enzyme thymidylate synthase (TS). In various studies [^{18}F]FLT has been proven to be useful in monitoring response to anti-cancer treatments (6,7). There are only limited reports on [^{18}F]FLT PET imaging concentrating on other proliferative tissues than tumors like the hematopoietic compartments. One study showed that [^{18}F]FLT PET can visualize bone marrow recovery after bone marrow transplantation in rats (8). And Ye et al. described that [^{18}F]FLT PET is capable of imaging the proliferative state of cells in aortic plaques and hematopoietic organs in mice, rabbit and men (9).

Here, we employed [^{18}F]FLT PET to non-invasively and longitudinally visualize the recovery of hematopoietic organs after chemotherapeutic treatment with gemcitabine in a mouse model.

MATERIALS AND METHODS

Animal model

Animal procedures were performed within the multi-centered QuIC-ConCePT study in accordance with the German Laws for Animal Protection and were approved by the animal care committee of the local government (North Rhine-Westphalia State Agency for Nature, Environment and Consumer Protection). During the experiments general health and body weight of the mice were monitored. 8-12 week old female NMRI nude mice (Janvier Labs) were used for the experiments. A total of n = 47 mice were employed in this study, which were initially used to monitor response of subcutaneous lung cancer xenografts to chemotherapy. Mice were treated with intraperitoneal injections of 100 mg/kg gemcitabine in 100 µL 0.9 % NaCl or 0.9 % NaCl vehicle control on d0 and d3. Analyses of d3 samples were performed after a single injection on d0. PET imaging was conducted according to the experimental schedule depicted in **Supplementary Fig. S1**. When performing BrdU flow cytometry or immunohistochemistry, 50 mg/kg BrdU *(*5-bromo-2'-deoxyuridine, B5002, Sigma-Aldrich) was injected intraperitoneally 6-8 h prior to cervical dislocation of the animal. Analysis of heparinized blood samples was performed with a Vet ABC^{TM} Animal Blood Counter (scil).

PET imaging

Synthesis of [^{18}F]FLT was performed as described previously (10). Emission scans were acquired with a quadHIDAC dedicated small animal PET camera (Oxford Positron Systems (11)) 70-90 min after injection of 10 MBq of the tracer. Mice were anesthetized with isoflurane inhalation (2 % in oxygen), and temperature was maintained by using a heating pad. A multimodal animal bed was used that was transferred to a computed tomography (CT, Siemens Inveon) or a magnetic

resonance (MR) tomograph (9.4 T, Biospec, Bruker, T2w imaging). This allowed coregistration with anatomical data with the help of fiducial markers.

After OPL-EM reconstruction (12) PET images were fused with either CT or MR images with the software Inveon Research Workspace 3.0 (Siemens Medical Solutions). Volumes of interest (VOIs) were drawn on manubrium sterni, femur, spleen, muscle, and liver guided by CT / MR images. [^{18}F]FLT accumulation was determined as $\%ID_{max}$/mL. We also calculated $\%ID_{mean}$/mL, SUV_{max}, SUV_{mean}, ratio to muscle (($\%ID_{max}$/mL)/($\%ID_{mean}$muscle/mL)) and ratio to liver (($\%ID_{max}$/mL)/($\%ID_{mean}$liver/mL)) to confirm that the mode of analysis does not alter the results. The respective data are depicted in **Supplementary Table S1**.

Immunohistochemistry

Spleen and femur were excised and fixed in 4 % paraformaldehyde. The bones underwent a decalcification procedure (incubation in 20 % EDTA for 4 weeks at 37 °C) prior to embedding in paraffin. 5 µm sections were cut from paraffin embedded tissue and stained overnight at 4 °C for either BrdU (AbD Serotech, OBT0030G, 1:100) or Ki67 (Abcam, ab16667, 1:100). Antibody binding was visualized with a respective secondary antibody labeled with 3,3'-diaminobenzidine (DAB). Images were acquired with a Nikon Eclipse 90i microscope and the NIS-Elements software package (Nikon). ImageJ (National Institutes of Health) was used for quantification of the specifically stained area after color deconvolution. The average of the DAB-positive area of 5-8 images at 20x resolution per section was determined.

Bone marrow cell isolation and BrdU flow cytometry

Bone marrow cells were isolated by flushing the cells of the femur in 5 mL PBS / 2 % BSA. The total cell number was determined by counting the cells in a Z2 coulter particle count and size analyser (Beckman Coulter). Thereafter, cells were pelleted by centrifugation and erythrocytes were lysed by incubation for 5 min with AKC lysis buffer (0.15 % NH_4Cl, 0.1 M EDTA, 1 mM $KHCO_3$, pH 7.4). After addition of 5 mL washing buffer (PBS / 2 % BSA) cells were centrifuged again. The cell pellet was then fixed in 70 % cold ethanol in PBS and stored at -20 °C. After washing, DNA was denatured by incubation with 400 µL 2 M HCl for 20 min. The cells were washed again and incubation for 2 min with 600 µL 0.1 M sodium tetraborate (pH 8.5) ensured a neutralization of the pH. After an additional washing step the cell pellet was incubated with 10 µL of anti-BrdU antibody (BD Pharmingen, # 556028) for 1 h. 250 µL 50 µg/mL propidium iodide were added 1 h before measuring the cells in a flow cytometer (FACSCalibur, Becton Dickinson). All steps were performed at room temperature and were followed by centrifugation (400 x g, 5 min).

Statistics

Box plots were used to visualize the median and the 25% and 75%iles. Whiskers represent minimum and maximum values. Mean and standard deviation were calculated as well and can be found in the **Supplementary Table S2** including numbers of samples analyzed. *P* values < 0.05 calculated by Mann-Whitney Rank Sum Test (Sigma Plot 13.0) were considered statistically significant.

RESULTS

When imaging tumor bearing nude mice after gemcitabine therapy by [^{18}F]FLT PET we noticed an atypical pattern of [^{18}F]FLT distribution within the body with clear accumulation in bone marrow and spleen (**Fig. 1**). In untreated or vehicle treated mice these organs could not be discriminated from background, whereas 2 d - 3 d after a single dose of gemcitabine, or d5 of gemcitabine therapy (i.e. 2 d after two doses of gemcitabine on d0 and d3), these organs clearly showed an enhanced uptake of [^{18}F]FLT (e.g. [^{18}F]FLT uptake in femur in $\%ID_{max}$/ml: baseline: 3.52 ± 0.59, d2: 6.25 ± 2.35†††,***, d3: 15.46 ± 6.58†††,*, d5: 9.99 ± 1.12††; ††: $P < 0.05$, †††: $P < 0.01$ relative to baseline; *: $P < 0.05$, ***: $P < 0.001$ relative to NaCl; see **Supplementary Table S2** for all numbers).

The bone marrow compartment and the spleen represent organs that are important for hematopoiesis, i.e. the production of new blood cellular components. Many chemotherapeutic agents, including gemcitabine, affect hematopoietic compartments, since the cells of these tissues are highly proliferating. After a while the hematopoietic organs recover, giving rise to new blood cells. We hypothesized that increased [^{18}F]FLT uptake represents recovery of hematopoietic organs after initial myelosuppression.

To analyze if gemcitabine exerts a myelosuppressive effect in our mouse model, we first performed blood count analysis (**Fig. 2**). We noticed a decrease of leukocytes (10^3 cells/ml NaCl vs. d5 gemcitabine: white blood cells: 6.5 ± 3.7 vs. 2.8 ± 1.3*, monocytes: 0.53 ± 0.43 vs. 0.05 ± 0.05**, granulocytes: 3.82 ± 2.84 vs. 0.95 ± 0.26**; *: $P < 0.05$, **: $P < 0.01$ relative to NaCl), indicating that gemcitabine indeed affects the cells responsible for the formation of peripheral blood cellular components. Other

blood cells were not affected at the time points investigated (see **Supplementary Table S3**).

Spleen weights as well as bone marrow cell counts were reduced 6 h or 1 d after gemcitabine (spleen-to-body weight: NaCl: 4.4 ± 1.3, 6 h gemcitabine: 3.1 ± 0.6*, d1 gemcitabine: 2.8 ± 0.7**; 10^6 bone marrow cells: NaCl: 20.2 ± 4.9, 6 h gemcitabine: 14.9 ± 1.4*, d1 gemcitabine: 7.8 ± 3.2***; *: $P < 0.05$, **: $P < 0.01$, ***: $P < 0.001$ relative to NaCl; **Fig. 3**), underlining that gemcitabine negatively effects these hematopoietic compartments. On d2, d3 and d5 of gemcitabine therapy, spleen weight was undistinguishable from NaCl treated controls, indicating recovery of this organ. The number of bone marrow cells was again decreased on d5.

Also immunohistochemistry of spleen tissue confirmed that gemcitabine exerted an effect on the cells giving rise to blood cellular components: the proliferation was significantly impaired 6 h and 1 d after drug administration (% Ki67-positive area: NaCl: 41.5 ± 9.8, 6 h gemcitabine: 5.6 ± 3.0*, d1 gemcitabine: 7.9 ± 4.4*; BrdU-positive area: NaCl: 36.6 ± 11.7, 6 h gemcitabine: 18.8 ± 9.8*, d1 gemcitabine: 5.5 ± 2.5**; *: $P < 0.05$, **: $P < 0.01$ relative to NaCl) and the proliferation receded to baseline levels on d2, d3 and d5 (**Fig. 4**). Proliferation of the bone marrow cells of the femur after gemcitabine treatment was affected in a similar manner (see **Supplementary Fig. S2**).

To more closely evaluate the proliferative status of the hematopoietic tissue upon gemcitabine therapy, we performed BrdU flow cytometry of the bone marrow cells to assess the number of cells in S-phase and performed propidium iodide staining to determine the cellular DNA content (**Fig. 5**). Analog to the immunohistochemistry of BrdU a significant drop in BrdU staining could be noted after 6 h (% BrdU-positive

cells: NaCl: 32.8 ± 4.7, 6 h gemcitabine: 6.9 ± 4.2, $P < 0.01$). Furthermore, propidium iodide incorporation revealed that the DNA of bone marrow cells 6 h after gemcitabine treatment appeared to be more fragmented, indicating apoptosis (% apoptotic cells: NaCl: 0.4 ± 0.4, 6 h: 1.6 ± 0.8, $P < 0.01$). On d2, d3 and d5 of gemcitabine therapy BrdU incorporation exceeded that of vehicle treated bone marrow cells up to 65 %, implying an increase of proliferation.

Conversely, proliferation of bone marrow cells as measured by flow cytometry on d1 of therapy was comparable to that of vehicle treated mice. This was in contradiction to the results obtained by the other experimental approaches employed, which demonstrated that also on d1 the myelosuppressive effect of gemcitabine is very prominent. This discrepancy can probably be explained by the fact that flow cytometry does not account for the absolute number of cells, but for the number of positive cells relative to the number of cells present. As can be seen on immunohistochemical sections (**Supplementary Fig. S2**) the absolute cell number is severely impaired, and the few remaining cells indeed are BrdU-positive. Low bone marrow cell numbers could also be directly noted by counting of bone marrow cells (**Fig. 3**).

In summary, with a panel of different *ex vivo* analyses we showed that bone marrow and spleen tissue were impaired early after gemcitabine administration, which was followed by a later recovery of these compartments.

DISCUSSION

Here, we demonstrate that gemcitabine exerts a myelosuppressive effect in a mouse model of cancer and that [^{18}F]FLT PET is able to non-invasively image the subsequent recovery of the hematopoietic organs *in vivo*.

Our [^{18}F]FLT PET imaging results showed substantial proliferation of the hematopoietic compartment if there was enough time for the tissue to recover after gemcitabine therapy (i.e. at least 2 d, **Fig. 1**). In a pilot study, we also observed accumulation of [^{18}F]FLT in bone marrow and spleen in mice 3 d after two doses of paclitaxel (see **Supplementary Fig. S3**). The latter finding implies that the preclinical observations made here for gemcitabine can also be transferred to other therapeutic approaches.

Our observations were corroborated by extensive *ex vivo* analyses of the proliferative status of the hematopoietic organs. The mass and proliferation of hematopoietic compartments was severely impaired early after application of a single dose of gemcitabine (after 6 h and 1 d), and apoptosis was increased. Hence, we directly showed that gemcitabine exerts a myelosuppressive effect. After 5 d we were able to show reduced leukocyte cell counts (**Fig. 2**). This indicator of myelosuppression, which is also frequently assessed in the clinic, is not directly timely linked to degradation of the bone marrow compartment. Lymphocytes are extremely sensitive and die in interphase. Hence, in a mouse model of radiotherapy, their number was reduced within the first week of therapy. In that experimental approach thrombocytopenia could be noted after 2-3 weeks and anemia after 2-3 months (13). Our results of reduced numbers of leukocytes are well in line with these data, whereas reduction of platelets or red blood cells can probably only be measured at later time points.

In our study, the hematopoietic organs recovered from d2 onwards as indicated by increased proliferation, spleen weight, and bone marrow cell number, respectively. However, it is interesting to note that the proliferation on d2, d3 and d5 as determined by *ex vivo* measurements was comparable to the proliferation state at baseline. On the other hand, [^{18}F]FLT PET imaging implied that the proliferation should be remarkably increased up to 4.5-fold in comparison to baseline. These results underline that [^{18}F]FLT should not be taken as a proliferation tracer *per se*. It is well recognized that its uptake can be influenced by a variety of factors, like presence of competing thymidine (14,15) or the balance of thymidine salvage and *de novo* pathway (16). It will be interesting to investigate, whether the latter differs between hematopoietic organs in an equilibrium state and in a recovery state. Analysis of the expression of TK1, TS and hENT1 at baseline and on d3 after gemcitabine did not point at an involvement of these proteins in the observed changes in [^{18}F]FLT uptake (**Supplementary Fig. S4**). However, it should be considered that expression levels are not necessarily directly related to enzyme or transporter activity.

Up to now, there are only limited possibilities to evaluate the proliferative state of hematopoietic organs. For instance, myelosuppressive effects of therapeutic approaches can be assessed by colony forming cell assays, employing hematopoietic stem cells isolated from bone marrow, cord blood or peripheral blood (17,18). Even though good correlations to clinically observed myelosuppression can be observed with regards to drug dose, no clear timely relations can be concluded from these *in vitro* studies. Also measurement of peripheral blood components does not provide timely information about the status of hematopoietic compartments. Another approach to assess myelosuppression is histological examination of bone marrow, requiring the collection of biopsies (19). Hence, there is need for a reliable, non-invasive method to assess the proliferation of hematopoietic compartments,

especially when employing novel therapy approaches. Therefore, we propose that [^{18}F]FLT PET should be considered and further explored in the clinical situation for that purpose.

There are a few clinical studies implying that [^{18}F]FLT accumulation indeed reflects proliferation of hematopoietic organs. Reduced [^{18}F]FLT uptake in the spinal bone marrow has been observed within the radiation field in head and neck cancer patients 5 d after 10 Gy radiotherapy (20) and in laryngeal carcinoma patients 1 month after 68 Gy radiotherapy (21). Moreover, [^{18}F]FLT reduction was shown to be related to radiation dose in head and neck cancer patients undergoing one week of chemoradiation (22). These reductions in tracer uptake presumably reflect reduced proliferation and can assist in further therapy planning. Furthermore, after platinum-based chemotherapy a substantial decrease in [^{18}F]FLT uptake could be noted in week two, which was followed by recovery in week four, reflecting the absence of chemotherapy between these time points. Uptake in spleen after four weeks even exceeded uptake prior to therapy, implying substantial proliferation (23). Also our data suggest that there needs to be a lag phase without therapy for the tissue to regenerate and accumulate high amounts of [^{18}F]FLT. This time frame might differ substantially between the different therapy approaches. Most likely the highest proliferation can be seen at the end of a treatment cycle. To further elucidate this issue, a retrospective systematic analysis of [^{18}F]FLT PET scans acquired for the assessment of tumor treatment response with respect to alterations in the hematopoietic compartments could be performed. Ideally, these imaging findings should be related to other established laboratory parameters, like peripheral blood counts. Better knowledge of the status of hematopoietic organs can help in improved understanding of the side effects of the applied treatment and thus facilitate future treatment planning in taking hematologic toxicity into account. Doing so with

established therapies will help to determine the value of [^{18}F]FLT PET for monitoring the proliferative state of hematopoietic organs. This will enable [^{18}F]FLT PET to be used for the visualization of myelosuppressive side effects of novel therapy approaches in a prospective manner.

Of note, even though there are clinical studies implying that [^{18}F]FLT PET is capable of visualizing the proliferation of hematopoietic compartments, these studies did not validate their observations by *ex vivo* tissue analyses. On contrary, our study indicates that changes in [^{18}F]FLT PET reflect changes in hematologic tissue biology. Therefore, our study provides the necessary link to employ [^{18}F]FLT PET for non-invasive assessment of hematopoietic proliferation and recovery after therapy.

ACKNOWLEDGEMENTS

We acknowledge Christine Bätza, Stefanie Bouma, Irmgard Hoppe, Nina Kreienkamp, Sarah Köster, Christa Möllmann, and Dirk Reinhardt for excellent technical assistance. We also acknowledge the Interdisciplinary Centre for Clinical Research (IZKF, core unit PIX), Münster, Germany for conducting the MR measurements, namely Prof. Dr. Cornelius Faber und Dr. Lydia Wachsmuth, and the PET measurements, namely Roman Priebe.

REFERENCES

1. Crawford J, Dale DC, Lyman GH. Chemotherapy-induced neutropenia: risks, consequences, and new directions for its management. Cancer. 2004;100:228–37.
2. Kuter DJ. Managing thrombocytopenia associated with cancer chemotherapy. Oncology (Williston Park). 2015;29:282–94.
3. Bohlius J, Weingart O, Trelle S, Engert A. Cancer-related anemia and recombinant human erythropoietin—an updated overview. Nat Clin Pract Oncol. 2006;3:152–64.
4. Panetta JC. Chemotherapeutic Effects on Hematopoiesis : A Mathematical Model. J Theor Med. 1998;I:209–21.
5. Paproski RJ, Ng AML, Yao SYM, Graham K, Young JD, Cass CE. The role of human nucleoside transporters in uptake of 3’-deoxy-3'-fluorothymidine. Mol Pharmacol. 2008;74:1372–80.
6. Tehrani OS, Shields AF. PET imaging of proliferation with pyrimidines. J Nucl Med. 2013;54:903–12.
7. Bollineni VR, Kramer GM, Jansma EP, Liu Y, Oyen WJG. A systematic review on [18F]FLT-PET uptake as a measure of treatment response in cancer patients. Eur J Cancer. 2016;55:81–97.
8. Awasthi V, Holter J, Thorp K, Anderson S, Epstein R. F-18-fluorothymidine-PET evaluation of bone marrow transplant in a rat model. Nucl Med Commun. 2010;31:152–8.
9. Ye Y-X, Calcagno C, Binderup T, Courties G, Keliher EJ, Wojtkiewicz GR, et al. Imaging Macrophage and Hematopoietic Progenitor Proliferation in Atherosclerosis. Circ Res. 2015;117:835–45.
10. Viel T, Schelhaas S, Wagner S, Wachsmuth L, Schwegmann K, Kuhlmann M,

et al. Early assessment of the efficacy of temozolomide chemotherapy in experimental glioblastoma using [18F]FLT-PET imaging. PLoS One. 2013;8:e67911.

11. Schäfers KP, Reader AJ, Kriens M, Knoess C, Schober O, Schäfers M. Performance evaluation of the 32-module quadHIDAC small-animal PET scanner. J Nucl Med. 2005;46:996–1004.
12. Reader AJ, Ally S, Bakatselos F, Manavaki R, Walledge RJ, Jeavons AP, et al. One-pass list-mode EM algorithm for high-resolution 3-D PET image reconstruction into large arrays. Ieee Trans Nucl Sci. 2002;49:693–9.
13. Mauch P, Constine L, Greenberger J, Knospe W, Sullivan J, Liesveld JL, et al. Hematopoietic stem cell compartment: acute and late effects of radiation therapy and chemotherapy. Int J Radiat Oncol Biol Phys. 1995;31:1319–39.
14. Zhang CC, Yan Z, Li W, Kuszpit K, Painter CL, Zhang Q, et al. [(18)F]FLT-PET imaging does not always “light up” proliferating tumor cells. Clin Cancer Res. 2012;18:1303–12.
15. Schelhaas S, Wachsmuth L, Viel T, Honess DJ, Heinzmann K, Smith D-M, et al. Variability of proliferation and diffusion in different lung cancer models as measured by 3’-deoxy-3'-18F-fluorothymidine PET and diffusion-weighted MR imaging. J Nucl Med. 2014;55:983–8.
16. McKinley ET, Ayers GD, Smith RA, Saleh SA, Zhao P, Washington MK, et al. Limits of [18F]-FLT PET as a biomarker of proliferation in oncology. PLoS One. 2013;8:e58938.
17. Pessina A, Albella B, Bayo M, Bueren J, Brantom P, Casati S, et al. Application of the CFU-GM assay to predict acute drug-induced neutropenia: an international blind trial to validate a prediction model for the maximum tolerated dose (MTD) of myelosuppressive xenobiotics. Toxicol Sci. 2003;75:355–67.

18. Yadav NK, Shukla P, Omer A, Singh RK. In-vitro hematological toxicity prediction by colony-forming cell assays. Toxicol Environ Health Sci. 2013;5:169–76.

19. Khalil F, Cualing H, Cogburn J, Miles L. The criteria for bone marrow recovery post-myelosuppressive therapy for acute myelogenous leukemia: a quantitative study. Arch Pathol Lab Med. 2007;131:1281–9.

20. Menda Y, Ponto LLB, Dornfeld KJ, Tewson TJ, Watkins GL, Gupta AK, et al. Investigation of the pharmacokinetics of 3’-deoxy-3'-[18F]fluorothymidine uptake in the bone marrow before and early after initiation of chemoradiation therapy in head and neck cancer. Nucl Med Biol. 2010;37:433–8.

21. Agool A, Slart RHJA, Thorp KK, Glaudemans AWJM, Cobben DCP, Been LB, et al. Effect of radiotherapy and chemotherapy on bone marrow activity: a 18F-FLT-PET study. Nucl Med Commun. 2011;32:17–22.

22. McGuire SM, Menda Y, Boles Ponto LL, Gross B, Buatti J, Bayouth JE. 3’-deoxy-3'-[^{18}F]fluorothymidine PET quantification of bone marrow response to radiation dose. Int J Radiat Oncol Biol Phys. 2011;81:888–93.

23. Leimgruber A, Moller A, Everitt SJ, Chabrot M, Ball DL, Solomon B, et al. Effect of Platinum-Based Chemoradiotherapy on Cellular Proliferation in Bone Marrow and Spleen, Estimated by 18F-FLT PET/CT in Patients with Locally Advanced Non-Small Cell Lung Cancer. J Nucl Med. 2014;55:1075–80.

FIGURE LEGENDS

Figure 1. PET imaging of gemcitabine treated mice revealed increased [^{18}F]FLT uptake in hematopoietic organs. Maximum intensity projections of emission scans acquired 70-90 min after tracer injection showed that the tracer accumulated in bone marrow and spleen starting from about d2 after drug administration. Quantification verified that this increased uptake pattern is reproducible. The black dots adjacent to the animals represent the coregistration landmarks. Subcutaneous tumors were also visible on the PET images. bl = baseline; white: NaCl control; grey: gemcitabine; *: $P < 0.05$, **: $P < 0.01$, ***: $P < 0.001$ relative to NaCl; †: $P < 0.05$, ††: $P < 0.01$, †††: $P < 0.001$ relative to baseline.

Figure 2. Hemogram analysis showed onset of low blood count after gemcitabine therapy. Heparinized blood was measured in a blood counter. *: $P < 0.05$, **: $P < 0.01$ relative to NaCl control.

Figure 3. Numbers of spleen and bone marrow cells were reduced early after gemcitabine therapy. Excised spleens were weighted and bone marrow (bm) cells flushed from the femur were counted as indicators for myelosuppression. *: $P < 0.05$, **: $P < 0.01$, ***: $P < 0.001$ relative to NaCl control.

Figure 4. Immunohistochemistry of spleen tissue revealed that proliferation was severely impaired after gemcitabine application. The DAB-positive area was quantified to assess the proliferative status of the tissue. *: $P < 0.05$, **: $P < 0.01$ relative to NaCl control. Scale bar = 100 µm.

Figure 5. Flow cytometry confirmed decreased proliferation early after gemcitabine application, which was accompanied by increased cell death after 6 h. BrdU-positive nuclei represent cells within the S-phase. Propidium iodide incorporation provides information on DNA content. Cells in the G_2/M phase possess duplicated DNA. 6 h after gemcitabine, an increased population of cells with fragmented DNA could be noted representing cells in $SubG_1$, i.e. cells undergoing cell death. *: $P < 0.05$; **: $P < 0.01$ relative to NaCl control.

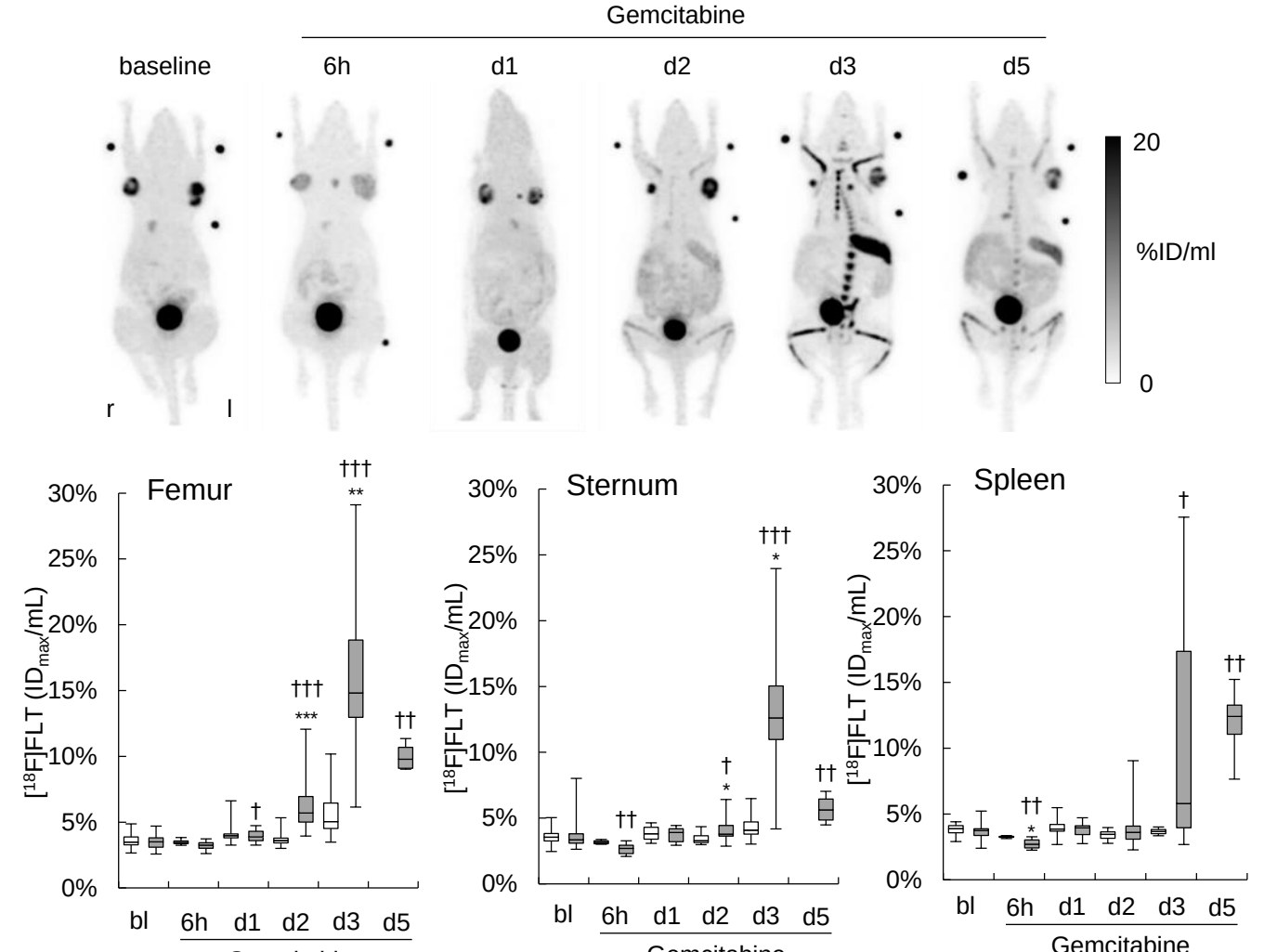

Figure 1

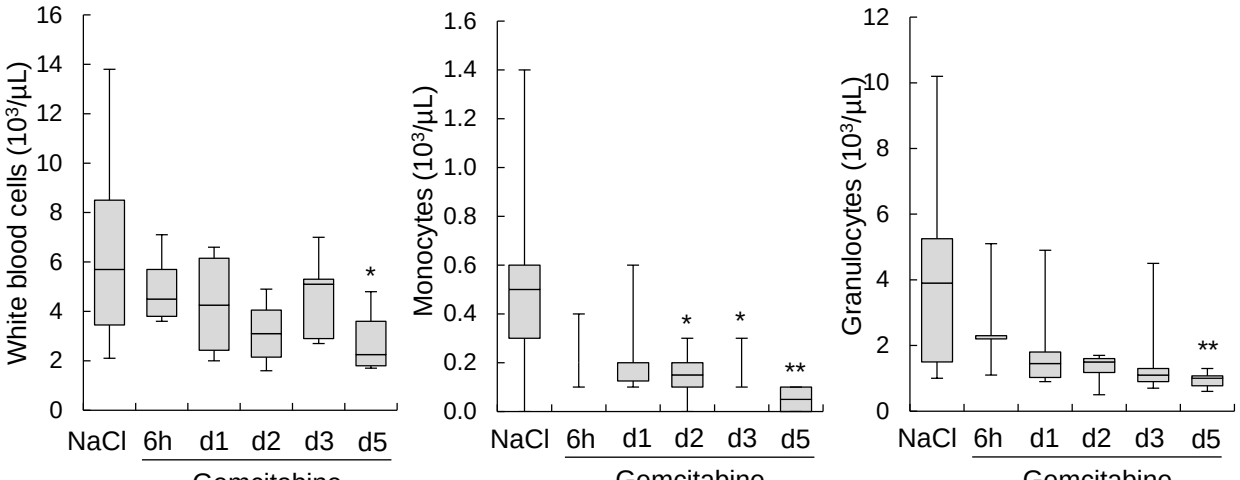

Figure 2

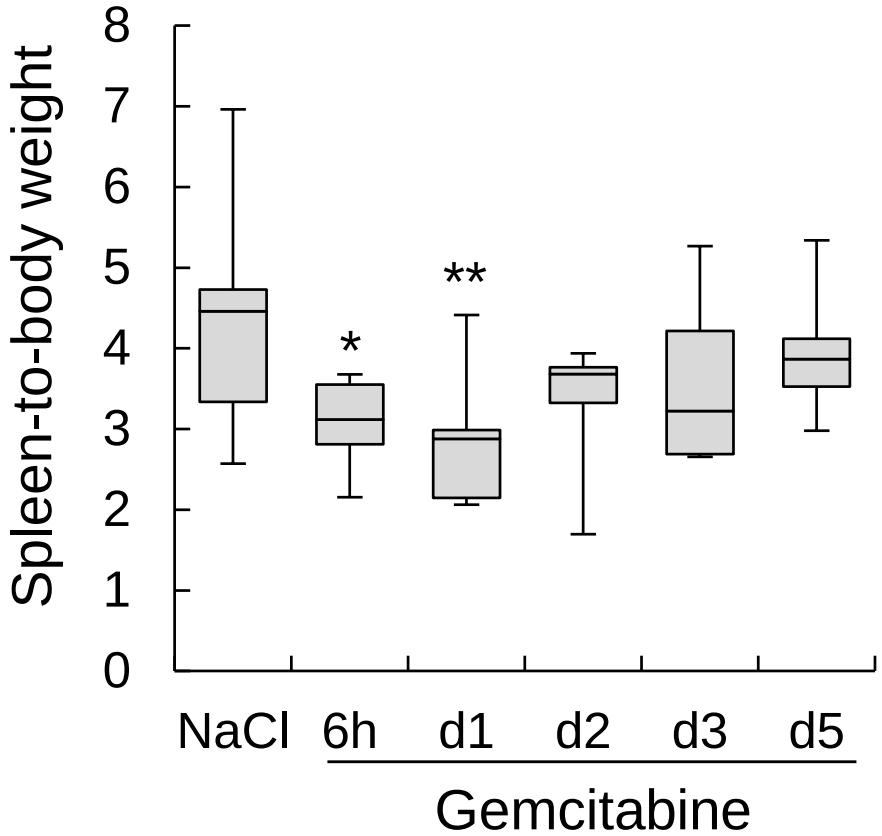

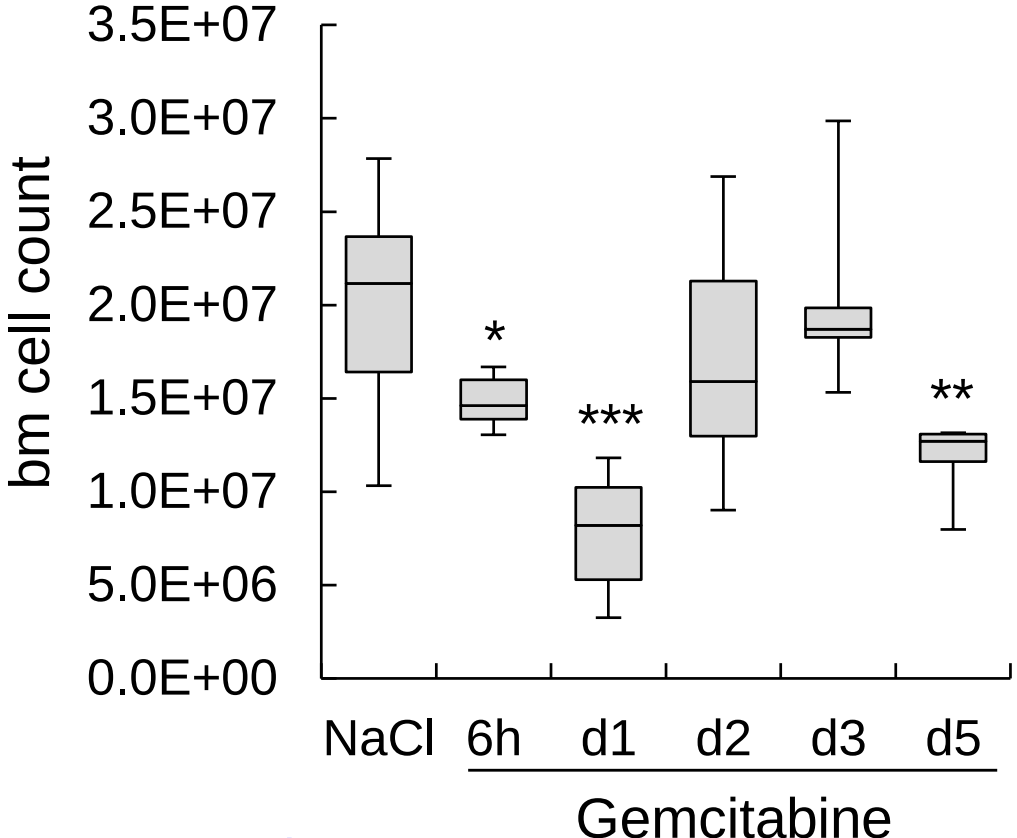

Figure 3

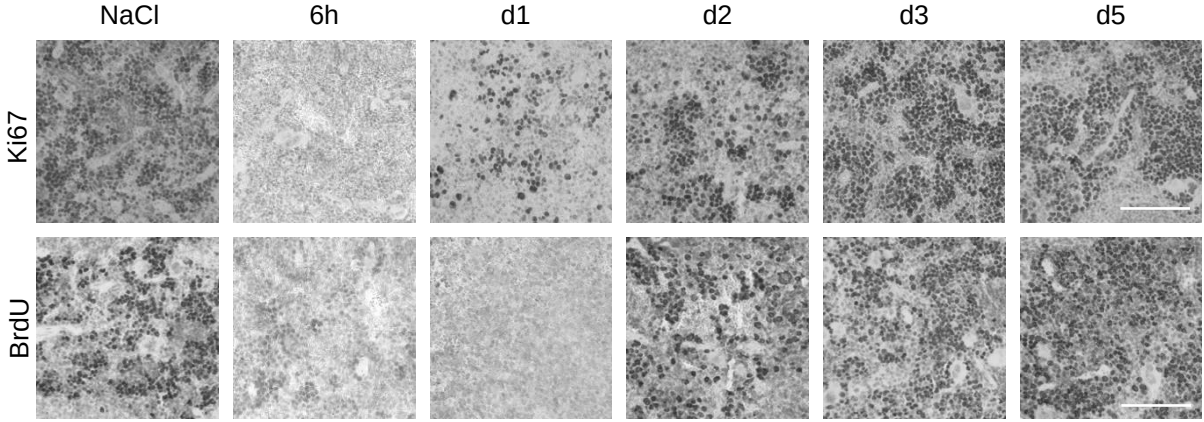

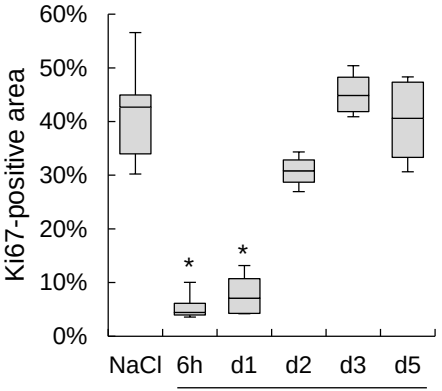

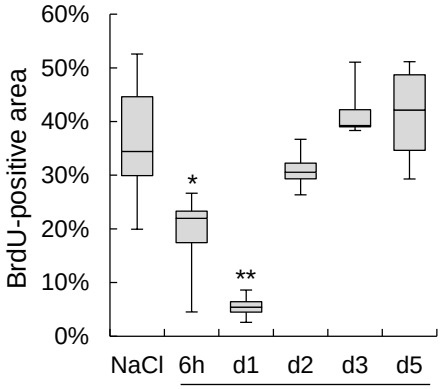

Figure 4

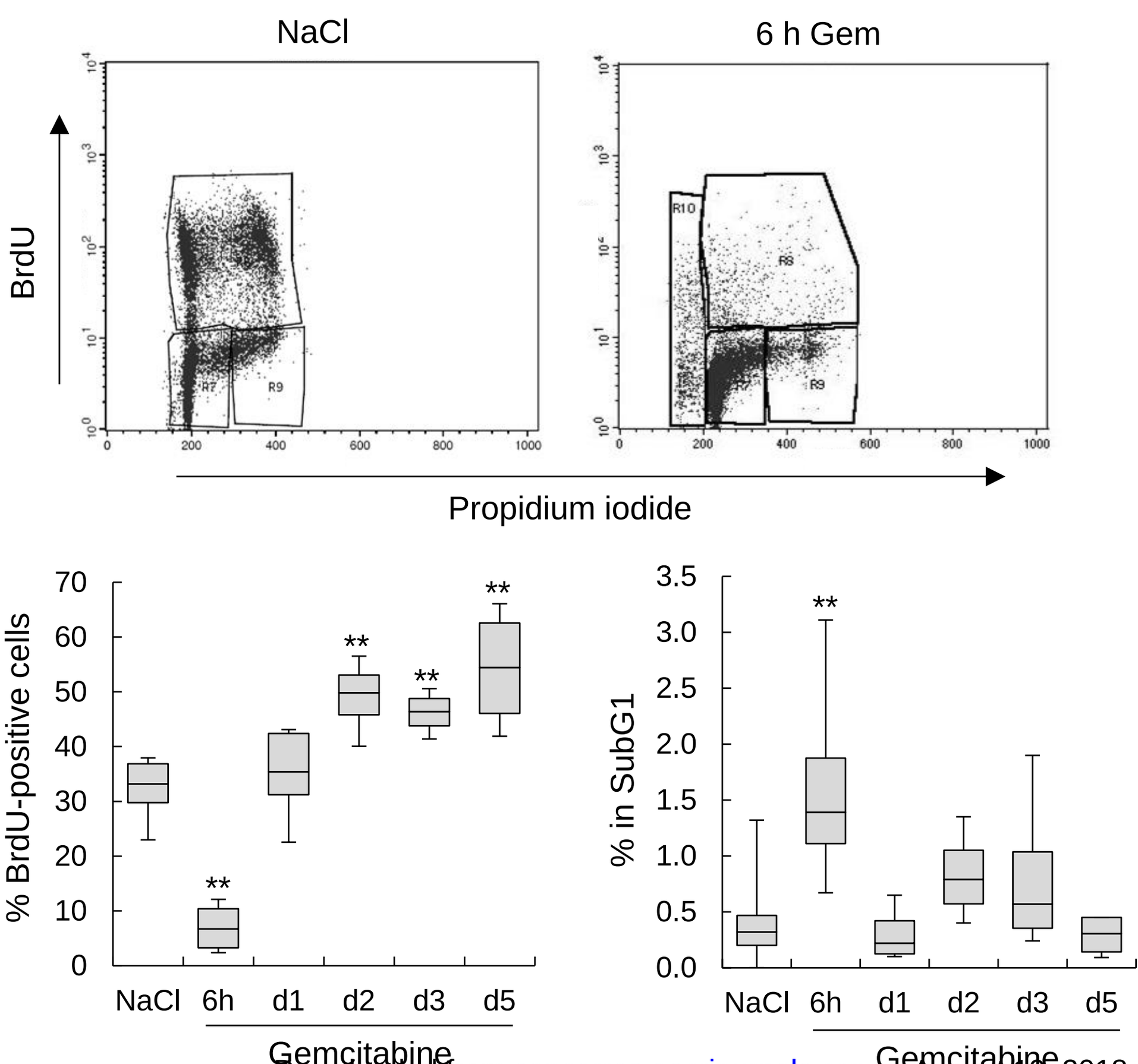

Figure 5

AACR American Association for Cancer Research

Cancer Research

The Journal of Cancer Research (1916–1930) | The American Journal of Cancer (1931–1940)

Preclinical evidence that 3'-Deoxy-3'-[18F]Fluorothymidine PET can visualize recovery of hematopoesis after gemcitabine chemotherapy

Sonja Schelhaas, Annelena Held, Nicole Bäumer, et al.

Cancer Res Published OnlineFirst October 20, 2016.